Modes of binding of guanosine monophosphates to ribonuclease T₁ – A computer-modelling study

P. V. Balaji, W. Saenger† and V. S. R. Rao*

Molecular Biophysics Unit, Indian Institute of Science, Bangalore 560 012, India
†Institute for Crystallography, Free University Berlin, Takustrasse 6, D-1000, Berlin 33, Germany

Computer-modelling studies on the modes of binding of the three guanosine monophosphate inhibitors 2'-GMP, 3'-GMP, and 5'-GMP to ribonuclease (RNase) T₁ have been carried out by energy minimization in Cartesian-coordinate space. The inhibitory power was found to decrease in the order 2'-GMP > 3'-GMP > 5'-GMP in agreement with the experimental observations. The ribose moiety was found to form hydrogen bonds with the protein in all the enzyme–inhibitor complexes, indicating that it contributes to the binding energy and does not merely act as a spacer between the base and the phosphate moieties as suggested earlier. 2'-GMP and 5'-GMP bind to RNase T₁ in either of the two ribose puckered forms (with C3'-endo more favoured over the C2'-endo) and 3'-GMP binds to RNase T₁ predominantly in C3'-endo form. The catalytically important residue His-92 was found to form hydrogen bond with the phosphate moiety in all the enzyme–inhibitor complexes, indicating that this residue may serve as a general acid group during catalysis. Such an interaction was not found in either X-ray or two-dimensional NMR studies.

RIBONUCLEASE (RNase) T₁ (EC 3.1.27.3), secreted by the fungus *Aspergillus oryzae*, is an endonuclease, whose sequence of 104 amino-acid residues is known[1]. It acts only on single-stranded RNA and hydrolyses the P–O5' phosphodiester bonds on the 3'-side of guanine nucleosides with very high specificity. A variety of physicochemical techniques like NMR and CD spectroscopy, UV difference spectroscopy, chemical modification and kinetic studies have been used [2–4] to elucidate the specific recognition of guanine by RNase T₁. Recent 1.9-Å resolution X-ray crystallographic studies of the Lys25- (ref. 5) and Gln25-RNase T₁-2'-GMP (ref. 6) complexes agree in general with each other regarding the conformation of the bound 2'-GMP molecule (C2'-*endo syn*) but differ in the nature of the hydrogen bonds between 2'-GMP and RNase T₁. The hydrogen-bonding scheme proposed for the RNase T₁-2'-GMP complex based on two-dimensional NMR spectroscopic studies[7] also differs significantly from each of the schemes proposed from X-ray studies (Table 1). A 2.6-Å-resolution X-ray crystallographic study of the RNase T₁-3'-GMP complex[8] showed that the main-chain polypeptide folding is very similar to that seen in the

Lys25-RNase T₁-2'-GMP complex[5]. This study could reveal only the hydrogen bonds between the base and the protein (Table 2), which are very similar to those observed in the Lys25-RNase T₁-2'-GMP complex. In contrast, 2D NMR studies[7] predicted that the structure of the RNase T₁-3'-GMP complex is more similar to that of the uncomplexed enzyme rather than to the RNase T₁-2'-GMP complex. The conformation of 3'-GMP in the RNase T₁-3'-GMP complex was not indicated by either the X-ray[8] or the 2D NMR[7] studies. However, ¹H NMR investigations[9] on the complexes of RNase T₁ with 2'-GMP, 3'-GMP and 5'-GMP have indicated that 2'-GMP and 3'-GMP adopt C3'-*endo syn* conformation and 5'-GMP adopts C3'-*endo anti* conformation when bound to the enzyme. Thus the puckering of the ribose moiety in the RNase

Table 1. Hydrogen-bonding scheme in the RNase T₁-2'-GMP complex.

	X-ray (Ref. 5)	X-ray (Ref. 6)	2D NMR (Ref. 7)	Present calculations (C2'-endo)
Guanine				
N1H	E46 OE1	E46 OE1	E46 OE1 N99 OD1	E46 OE1
N2H	E46 OE2 N98 O	N98 O	N99 OD1	E46 OE2 N98 O
O6	N44 N–H Y45 N–H	N44 N	N44 N–H Y45 N–H	N44 N–H Y45 N–H
N7	N43 N–H	N43 N–H N43 HD2	N44 HD2	N43 N–H N43 HD21
Ribose				
O2'				H40 HE2
O3'			H40 HE2 N98 HD2	
O4'			N43 HD2	
O5'			N98 HD2	
O5'H			Y45 OH	N98 OD1
Phosphate				
O1	Y38 HH H40 HE2 E58 OE2		N98 HD2	N36 HD21
O2			R77 NE	Y38 HH E58 HE2 R77 HE2
O3		Y38 HH E58 HE2 R77 NH2	Y38 HH H40 HE2	H92 HE N98 HD22

Amino-acid residues of RNase T₁ are indicated by the single-letter code for amino acids and the residue number.

Table 2. Hydrogen-bonding scheme in the RNase T_1-3'-GMP complex.

	X-ray (Ref. 8)	2D NMR (Ref. 7)	Present calculations	
			C2'-endo	C3'-endo
Guanine				
N1H	E46 OE1	E46 OE1 E46 OE2 N99 OD1	E46 OE1	E46 OE1
N2H	E46 OE2 N98 O	N99 OD1	E46 OE2 N98 O	E46 OE2 N98 O
O6	N44 N-H Y45 N-H	Y42 HH E46 N-H F100 N-H	N44 N-H Y45 N-H	N44 N-H Y45 N-H
N7	N43 N-H	Y42 HH	N43 N-H N43 HD21	N43 N-H
Ribose				
O2'		Y38 HH	E58 HE2	
O2'H		E58 OE2		
O4'		N43 HD2		
O5'		N98 HD2	N98 HD21	H92 HE2
O5'H				N98 OD1
Phosphate				
O1		N36 N-H H40 HE2	N36 HD21 Y38 HH	N36 HD21 Y38 HH R77 HH21
O2			R77 HH21 H92 HE2	N36 HD22 H40 HE2
O3		S35 HG		R77 HE
O3H		N36 OD1 Y38 OH		E58 OE1

Amino-acid residues of RNase T_1 are indicated by the single-letter code for amino acids and the residue number.

T_1-2'-GMP complex seems to be different in solution from that observed in the solid state.

Preliminary computer-modelling studies[10] were carried out on the complexes of RNase T_1 with 2'-GMP, 3'-GMP and 5'-GMP by energy minimization in torsion-angle space recently. Though the results could explain many experimental observations, they were slightly at variance with the conclusions drawn from ^{1}H NMR studies[9] regarding the conformation assumed by 3'-GMP and 5'-GMP when bound to RNase T_1. The proposed hydrogen-bonding scheme is also different from that proposed on the basis of 2D NMR studies[7]. It was assumed in these modelling studies that the backbone conformation will be the same in all the three RNase T_1-GMP complexes as that observed in the RNase T_1-2'-GMP complex[10]. Though the local mobility within the RNase T_1 molecule, as represented by the mean crystallographic temperature factors of both the backbone and side-chain atoms, is different in the two X-ray crystal structure studies of the RNase T_1-2'-GMP complex[5,6], especially around the residue Asp-49, both studies indicated large fluctuations in the N-terminal and the loop regions compared to the α-helical and β-pleated-sheet regions and the inhibitor-binding site. In view of this, energy minimization of the three RNase T_1-GMP complexes was carried out in Cartesian-coordinate space by relaxing all the bonds,

bond angles and main-chain and side-chain torsion angles.

Methods of calculation

The low-energy conformers obtained by energy minimization in torsion-angle space[10] were used as starting points for energy minimization in Cartesian-coordinate space. The total conformational energy, which includes the intramolecular interaction energy of the protein and the ligand (comprising bond stretching, bond-angle bending, van der Waals, electrostatic, hydrogen-bonding, and normal and improper torsion potential terms) and intermolecular interaction energy between the enzyme and the inhibitor, was calculated using the expression

$$E_{tot} = E_{vw} + E_{ele} + E_{tor} + E_{imptor} + E_{hb} + E_{bl} + E_{ba}.$$

The electrostatic (E_{ele}), hydrogen-bond (E_{hb}), and van der Waals (E_{vw}) contributions were evaluated using the functions and the parameters described earlier[10]. The partial atomic charges used in these calculations for the amino-acid residues were taken from ref. 10, and the charges for the inhibitor atoms are shown in Table 3. A bond torsional model was used for evaluating the torsional potential (E_{tor}). Improper torsion potential (E_{imptor}) was used to maintain planarity and to avoid racemization at chiral centres. Bond lengths and bond angles were restrained to their equilibrium values by the use of harmonic potential functions (E_{bl} and E_{ba}). The form of the function and the parameters used are the same as those given by Weiner et al.[11,12]

All the amino-acid residues in the protein were

Table 3. Partial atomic charges (in e.c.u.) for GMP nucleotides.

Guanine			Ribose		
			2'-GMP	3'-GMP	5'-GMP
N1	-0.2139	C1'	0.2470	0.2388	0.2409
C2	0.3815	H1'	-0.0340	-0.0540	-0.0455
N3	-0.3272	C2'	0.1453	0.1135	0.1209
C4	0.2117	H2'	-0.0064	-0.0277	-0.0355
C5	-0.1020	C3'	0.1332	0.1631	0.1435
C6	0.3529	H3'	-0.0137	-0.0385	-0.0012
N7	-0.1652	C4'	0.1146	0.1303	0.1248
C8	0.1342	H4'	0.0233	0.0383	-0.0010
N9	-0.1202	O4'	-0.2672	-0.2658	-0.2379
N1H	0.1205	O2'	-0.3014	-0.2398	-0.2550
N2	-0.2474	O2'H	xx	0.1070	0.1182
N2H	0.1357	O3'	-0.2365	-0.3036	-0.2550
O6	-0.3890	O3'H	0.1056	xx	0.1182
C8H	-0.0128	C5'	0.1445	0.1309	0.1480
		H5'	-0.0203	0.0106	-0.0212
		O5'	-0.2601	-0.2601	-0.2811
		O5'H	0.1084	0.1084	xx
		P	0.3730	0.3730	0.3730
		PO1	-0.4749	-0.4749	-0.4749
		PO2	-0.4749	-0.4749	-0.4749
		PO3	-0.3356	-0.3356	-0.3356
		PO3H	0.1559	0.1559	0.1559

considered for energy minimization. A united-atom model for the protein and an all-atom model for the inhibitors were used (Figure 1). A residue-based nonbonded cutoff of 10 Å was used for calculating the intramolecular nonbonded energy of the protein, i.e. interactions were considered only between those residues whose atoms are within 10 Å from each other. For each residue, the list of other residues within the cutoff distance was updated at the end of every 200 iterations of minimization. All the calculations were carried out in double-precision arithmetic. A modification of the conjugate gradient algorithm as suggested by Shanno[13] was used for minimization, and minimization was terminated when the root-mean-square (rms) gradient was less than $0.01 \, \text{kcal mol}^{-1} \, \text{Å}^{-1}$.

Comparison of protein structures

For determining the rms shifts in the positions of the main-chain and the side-chain atoms of the energy-minimized RNase T_1-2'-GMP (C2'-endo) complex relative to the 1.9-Å-resolution X-ray crystallographic structure of the Lys25-RNase T_1-2'-GMP complex, the two structures were first superposed optimally. This involves translation and rotation of the energy-minimized structure with respect to the X-ray structure. The optimal translation is that which brings the mean positions, i.e. the centroids, of the two structures into coincidence. Hence the coordinates of the two structures were first transformed into a frame of reference whose origin is at the centroid of the X-ray structure. Next, the energy-minimized structure was rotated with

reference to the X-ray structure using the three Eulerian rigid-body rotation angles. The rms distance between the main-chain atoms (N, CA and C') of the two structures was then minimized as a function of these three rigid-body rotation angles.

Results and discussion

The minimum-energy conformer of the RNase T_1-2'-GMP (C2'-endo) complex obtained from the present calculations was compared with the X-ray crystallographic structure of the Lys25-RNase T_1-2'-GMP complex by least-squares superposition. A stereo view of the protein main-chain atoms before and after energy minimization is shown in Figure 2,a and that of the active-site residues and the inhibitor 2'-GMP in Figure 2,b. From these it can be seen that the deviations in the main-chain atom positions in the interior of the protein and the inhibitor-binding site are minimal whereas they are large in the N-terminal and loop regions. Such large deviations were also observed in molecular-dynamics simulations of RNase T_1 and the complex of RNase T_1 with 2'-GMP carried out in vacuum[14-18]. But when these molecular-dynamics simulations were carried out with an 18-Å water sphere around the protein, only the fluctuations observed at the N-terminal and loop regions were affected significantly, but not those observed in the interior of the protein or the inhibitor-binding region. This is to be expected since the X-ray crystallographic study of the Lys25-RNase T_1-2'-GMP complex showed that the inhibitor-binding site is part of an apparently underhydrated surface portion mainly due to the less hydrophilic nature of the amino-acid residues constituting this region[5]. Thus the deviations predicted from the present study in the interior of the protein molecule and in the inhibitor site reflect the changes in the protein due to inhibitor binding even though the solvent molecules are not treated explicitly.

RMS shifts in the positions of all the backbone and side-chain atoms in the three RNase T_1-GMP complexes from the X-ray crystallographic structure of Lys25-RNase T_1-2'-GMP are shown in Figure 3 and rms shifts for the active-site residues in Tables 4 and 5. In general, the movement of the amino-acid residues directly involved in binding and catalysis appears to be concerted and these residues deviate from the initial conformation mainly to form better hydrogen bonds with the bound inhibitor. On the other hand, the residues away from the active site move mainly to relieve the unfavourable steric interactions present in the reported X-ray structure. The deviations in the positions of both the main-chain and the side-chain atoms of the amino-acid residues around Asp-49 are comparatively less (Figure 3). It is interesting to note that the temperature-factor values for Asp-49 obtained
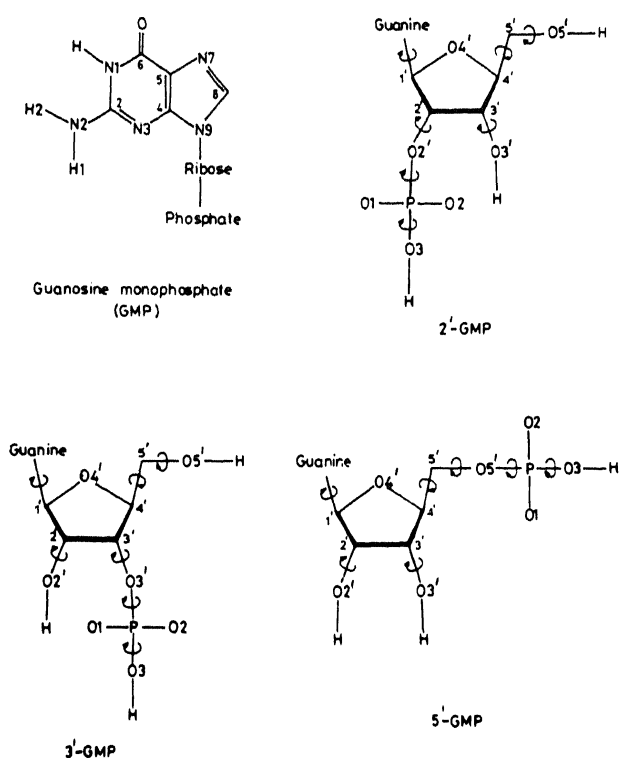

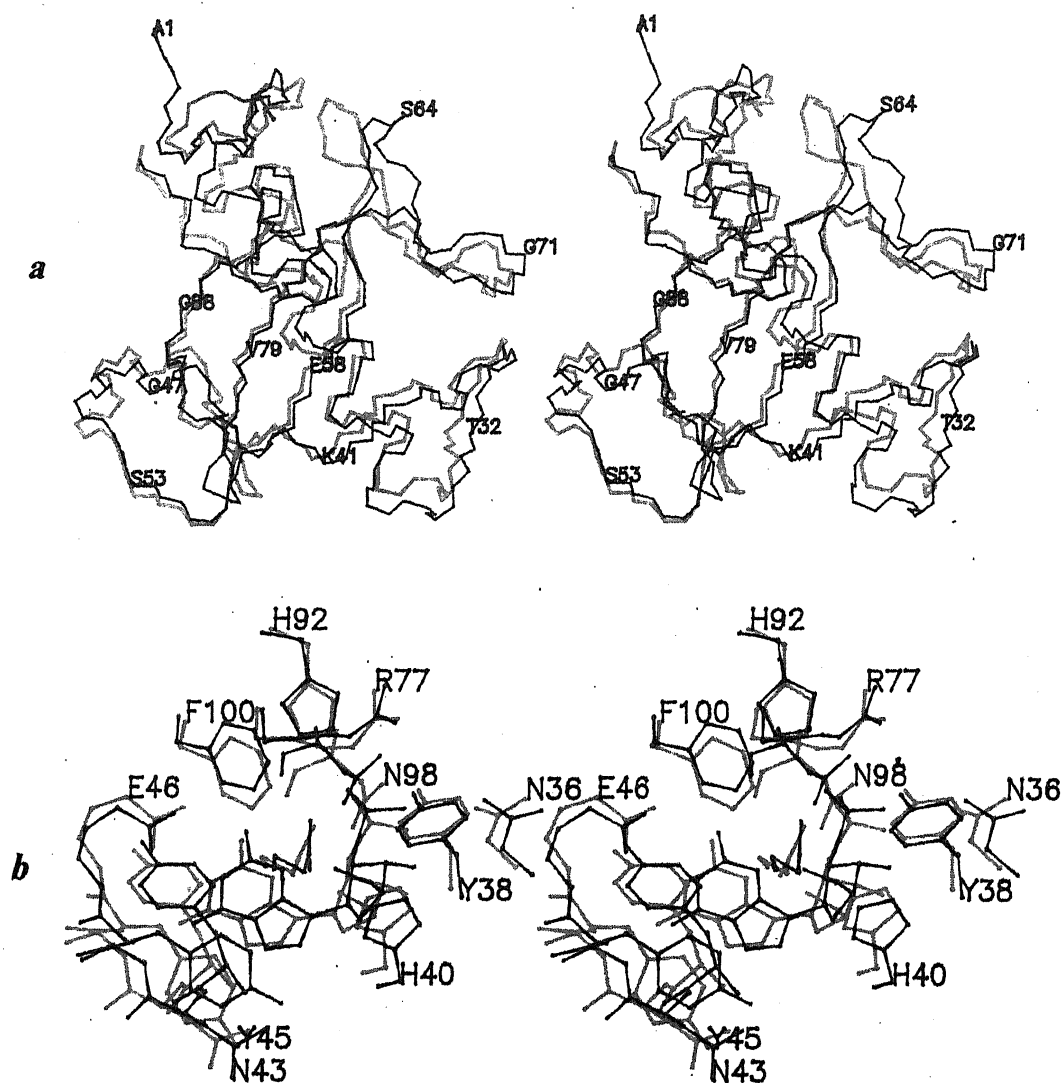**Figure 1.** Schematic diagrams of 2'-GMP, 3'-GMP and 5'-GMP.

Figure 2. Least-squares superposition of the main-chain atoms of the X-ray crystallographic structure of the Lys25-RNase T_1-2'-GMP complex (green) and the energy-minimized structure of the RNase T_1-2'-GMP (C2'-endo) complex (red): *a*, backbone atoms (N, CA, C'); *b*, active-site residues and the inhibitor 2'-GMP.

by the X-ray crystallographic study of Lys25-RNase T_1-2'-GMP complex are very high, indicating high mobility for this residue. But the temperature-factor values for the same residue obtained by X-ray studies of Gln25-RNase T_1-2'-GMP complex did not show any such large mobility for this residue, in agreement with the results obtained from the present calculations. These studies also indicate that some of the backbone atoms move by more than 1 Å (Figure 3 and Tables 4 and 5). Such deviations seem to affect the relative conformational energies of the RNase T_1–inhibitor complexes and the hydrogen-bonding scheme proposed from energy minimization studies in torsion-angle space[10].

Tables 1 and 2 show that the hydrogen-bonding scheme predicted from the present calculations for the RNase T_1-2'-GMP and the RNase T_1-3'-GMP complexes agrees better with those proposed from the X-ray crystallographic studies[5,6] rather than the 2D NMR

studies[7]. The orientation of the base in the theoretically predicted RNase T_1-2'-GMP (C2'-endo) complex is nearly the same as that observed in the X-ray crystallographic structure of the Lys25-RNase T_1-2'-GMP complex (Figure 2,b), but the ribose-phosphate conformation is slightly different. The number of hydrogen bonds between the base and the enzyme predicted here is slightly higher than the numbers reported from either of the two crystal-structure studies (Table 1)[5,6]. However, the present calculations indicate that all the hydrogen bonds proposed between the guanine base and the enzyme in the complex of 2'-GMP with both Gln25- and Lys25-RNase T_1 are possible, as revealed in the preliminary computer-modelling studies[10]. The ribose O2' and O5'H atoms can form hydrogen bonds with His-40 HE2 and Asn-98 OD1 of the protein respectively. The interaction between Asn-98 side chain and 2'-GMP predicted from the present study was not indicated by either of the two X-ray crystallographic
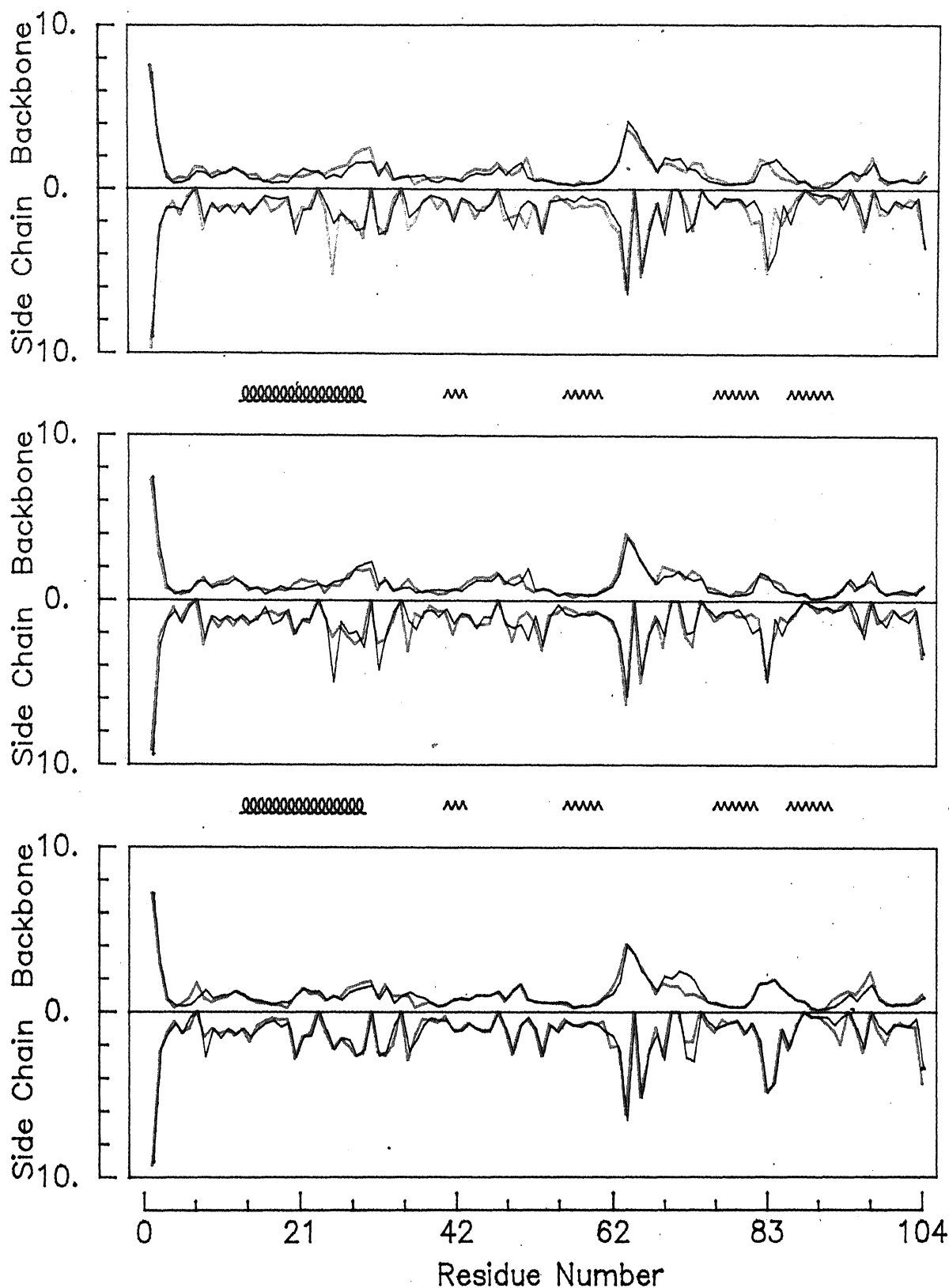
Figure 3. RMS shifts (Å) in the positions of the backbone and side-chain atoms in the energy-minimized structures of RNase T_1-2'-GMP (top panel), RNase T_1-3'-GMP (middle panel), and RNase T_1-5'-GMP (lower panel) complexes relative to the X-ray crystallographic structure of the Lys25-RNase T_1-2'-GMP complex (ribose pucker: C2'-*endo*, green; C3'-*endo*, red). Regions of α-helix and β-sheet are indicated between the panels.

studies[5,6]. However, such an interaction between the Asn-98 side chain and the ribose-phosphate moiety of 2'-GMP was reported in the 2D NMR study[7].

The conformational angles of 2'-GMP and 3'-GMP in the minimum-energy complexes of these inhibitors with RNase T_1 obtained from the present calculations are given in Table 6. Stereo diagrams of the active-site residues of the enzyme and the inhibitor in these two enzyme–inhibitor complexes in both the ribose puckers are shown in Figure 4,a–d. The hydrogen bonds

Table 4. RMS shifts (Å) in the positions of the main-chain atoms of the active-site residues in the RNase T_1–GMP complexes relative to the X-ray data for the RNase T_1–2'-GMP complex.

Amino-acid residue	2'-GMP		3'-GMP		5'-GMP	
	C2'-endo	C3'-endo	C2'-endo	C3'-endo	C2'-endo	C3'-endo
Ser-35	0.738	0.821	0.781	1.279	1.187	0.955
Asn-36	0.781	0.316	0.482	0.779	0.954	0.276
Ser-37	0.838	0.554	0.557	0.500	0.835	0.475
Tyr-38	0.472	0.677	0.627	0.540	0.521	0.581
His-40	0.643	0.717	0.607	0.428	0.467	0.378
Tyr-42	0.456	0.522	0.570	0.724	0.821	0.764
Asn-43	0.809	0.981	0.935	1.126	0.745	0.708
Asn-44	0.969	1.236	1.217	1.381	0.994	0.988
Tyr-45	0.905	1.199	1.215	1.403	0.996	1.000
Glu-46	0.931	1.137	1.180	1.356	0.994	1.007
Glu-58	0.352	0.498	0.395	0.367	0.387	0.312
Arg-77	0.307	0.511	0.408	0.521	0.369	0.382
His-92	0.412	0.460	0.296	0.363	0.345	0.772
Asn-98	0.748	0.691	0.656	0.861	0.748	0.983
Phe-100	0.544	0.515	0.546	0.515	0.446	0.363

Table 5. RMS shifts (Å) in the positions of the side-chain atoms of the active-site residues in the RNase T_1–GMP complexes relative to the X-ray data for the RNase T_1–2'-GMP complex.

Amino-acid residue	2'-GMP		3'-GMP		5'-GMP	
	C2'-endo	C3'-endo	C2'-endo	C3'-endo	C2'-endo	C3'-endo
Ser-35	1.742	2.510	1.293	3.086	2.356	2.880
Asn-36	1.311	1.962	1.757	0.804	1.709	1.392
Ser-37	0.731	0.839	0.705	1.049	0.788	0.441
Tyr-38	0.425	0.420	0.590	0.337	0.388	0.487
His-40	0.756	0.630	0.539	0.646	0.511	0.256
Tyr-42	0.573	0.714	0.800	0.975	1.147	1.084
Asn-43	0.787	0.817	0.916	0.953	0.723	0.686
Asn-44	1.291	1.756	1.673	1.531	1.033	0.968
Tyr-45	1.307	1.100	0.998	1.458	1.118	1.214
Glu-46	0.885	0.967	1.042	1.419	1.067	1.189
Glu-58	0.408	0.976	0.780	0.833	0.885	0.768
Arg-77	0.536	0.686	0.675	0.942	0.828	0.485
His-92	0.465	0.451	0.591	0.656	0.779	1.109
Asn-98	1.113	1.480	1.123	1.315	0.887	1.196
Phe-100	0.662	0.757	0.578	0.505	0.769	0.947

between the guanine base and the protein in both RNase T_1–2'-GMP and RNase T_1–3'-GMP complexes are the same, and the base orientation is also very similar in the two complexes. It can also be seen from Figure 3 that there is no significant change in the protein backbone conformation in the two enzyme–inhibitor complexes, especially in the base-binding site. The 2.6-Å-resolution X-ray crystallographic study of the RNase T_1–3'-GMP complex corroborates the conclusion drawn from the present study that the overall polypeptide-chain folding in the RNase T_1–3'-GMP complex is very similar to that found in the RNase T_1–2'-GMP complex rather than to that in guanosine-free RNase T_1, which differs in the base-recognition site[19]. Thus the results obtained from the present studies corroborate the conclusions drawn from the X-ray diffraction studies but disagree with the 2D NMR studies.

The conformation of 5'-GMP in its minimum-energy complex with RNase T_1 obtained from the present

calculations is given in Table 6 and the proposed hydrogen-bonding scheme in Table 7. Stereo diagrams of the active-site residues of RNase T_1 and the inhibitor in the RNase T_1–5'-GMP complex in both the ribose puckers are shown in Figure 4,e,f. It can be seen from Figure 4,a–f that the base-binding site mainly comprises the residues Tyr-42, Asn-43, Asn-44, Tyr-45, Glu-46, Asn-98 and Phe-100 in all the three RNase T_1–inhibitor complexes. The hydrogen bond between N98 O and N2H1 of guanine in the RNase T_1–3'-GMP (C3'-endo) complex, and the hydrogen bonds of O6 of guanine with N44 N–H and Y45 N–H and N7 of guanine with N43 NH in the RNase T_1–5'-GMP (C3'-endo) complex proposed from the present study were not revealed by the preliminary computer-modelling studies[10] even though the base-binding site and the orientation of the base are nearly the same in all the three enzyme–inhibitor complexes. It can be seen from Table 7 that guanine N1H is hydrogen-bonded to Glu-46 OE1 in all the cases. Guanine 2-NH_2 forms two hydrogen bonds:

Table 6. Total energy and conformational angles of 2'-, 3'- and 5'-GMP in the minimum-energy conformers of their complexes with RNase T_1.

Initial ribose pucker	C2'-endo			C3'-endo		
Inhibitor	2'-GMP	3'-GMP	5'-GMP	2'-GMP	3'-GMP	5'-GMP
Conformational angles (deg)						
C4–N9–C1'–O4'	70	60	−76	157	10	−69
C3'–C4'–C5'–O5'	75	71	−159	65	−68	−178
C3'–C2'–O2'–O2'H	—	−46	179	—	−75	−65
C2'–C3'–O3'–O3'H	81	—	59	71	—	62
C4'–C5'–O5'–O5'H	−77	41	—	65	−77	—
C1'–C2'–O2'–P	−167	—	—	66	—	—
C4'–C3'–O3'–P	—	−159	—	—	162	—
C4'–C5'–O5'–P	—	—	−84	—	—	−179
CX'–OX'–P–O3*	−57	75	−75	9	70	−108
OX'–P–O3–O3H*	−26	171	81	−107	−75	−56
Pseudorotation phase angle P (deg)	149.2	129.2	164.4	−3.8	11.9	8.8
H8–H1' distance (Å)	2.5	2.6	3.8	3.1	2.8	3.8
Energy (kcal mol^{-1})						
Ligand	−25.9	−27.3	−17.6	−19.5	−28.2	−20.8
Protein	−179.8	−187.6	−185.4	−179.3	−180.8	−181.5
Interaction	−146.7	−130.2	−135.7	−156.3	−144.0	−137.5
Total	−352.4	−345.2	−338.7	−355.0	−353.0	−339.8
Normalized energy†	−318.3	−311.5	−303.4	−320.9	−319.3	−304.5

*X = 2 in 2'-GMP, 3 in 3'-GMP, and 5 in 5'-GMP.

†Normalized enery = Total energy − energy of the isolated inhibitor molecule (−34.1 kcal mol^{-1} for 2'-GMP, −33.7 kcal mol^{-1} for 3'-GMP, and −35.3 kcal mol^{-1} for 5'-GMP).

one with Glu-46 OE2 and the second with Asn-98 O. O6 of the base accepts a hydrogen bond each from Asn-44 N–H and Tyr-45 N–H. N7 forms a hydrogen bond with both Asn-43 N–H and Asn-43 HD21 in all the complexes. However, the N7–Asn-43 HD21 hydrogen bond is not possible in the complexes of RNase T_1 with 3'-GMP (C3'-endo) and 5'-GMP (C3'-endo).

The ribose moiety of all the three inhibitors in both C2'-endo and C3'-endo puckered conformations forms a hydrogen bond with the Asn-98 side-chain amide group. A second hydrogen bond is also possible with one of the amino-acid residues Asn-36, His-40, Glu-58 or His-92 (Table 7). This suggests that the ribose moiety does not act merely as a spacer between the base and the phosphate to ensure proper disposition between them for binding, as indicated earlier[9], but also contributes significantly to the stability of the enzyme–inhibitor complex.

Table 7 shows that the phosphate group always prefers to bind in the same site of the protein comprising the residues Asn-36, Tyr-38, His-40, Glu-58, Arg-77, His-92 and Asn-98 in all the three enzyme–inhibitor complexes. The hydrogen bond between the side-chain amide group of Asn-36 and phosphate is possible in all the enzyme–inhibitor complexes except the RNase T_1–5'-GMP (C2'-endo) and RNase T_1–2'-GMP (C3'-endo) complexes. Although the His-40 side chain is near the phosphate group in all the complexes, hydrogen bond formation between them is possible only in the RNase T_1–3'-GMP (C3'-endo) complex. Interestingly, the present calculations predict that His-

92, which was shown to be important for catalysis by chemical modification and other physicochemical studies[2−4], forms at least one hydrogen bond with the phosphate group in all the complexes except in the RNase T_1–3'-GMP (C3'-endo) complex. Though His-92 was found to be present in the phosphate-binding site in the complexes of 2'-GMP with both Gln25- and Lys25-RNase T_1, no hydrogen bond was reported between His-92 and the phosphate group from these X-ray diffraction[5,6] or the 2D NMR studies[7].

The standard free energies of binding of 2'-, 3'- and 5'-GMP to RNase T_1 have been measured by different workers by gel filtration, UV difference-spectroscopic and kinetic studies but the values reported from these studies[2,20−23] differ significantly. These variations appear to be beyond the deviations expected for the differences in experimental conditions and techniques. But qualitatively, all these studies indicate that the inhibitory power decreases in the order 2'-GMP > 3'-GMP > 5'-GMP, which is in agreement with the energy values obtained from the present study (Table 6). Though the earlier computer-modelling studies also indicated the same order, the relative energy differences are different from those obtained in the present study.

Table 6 shows that the total conformational energy difference between the C2'-endo and C3'-endo pucker forms of the RNase T_1–2'-GMP and RNase T_1–5'-GMP complexes is very small. Thus 2'-GMP and 5'-GMP can bind to RNase T_1 in either C2'-endo or C3'-endo ribose pucker forms and exist in significant amounts in both puckered forms in solution, with C3'-
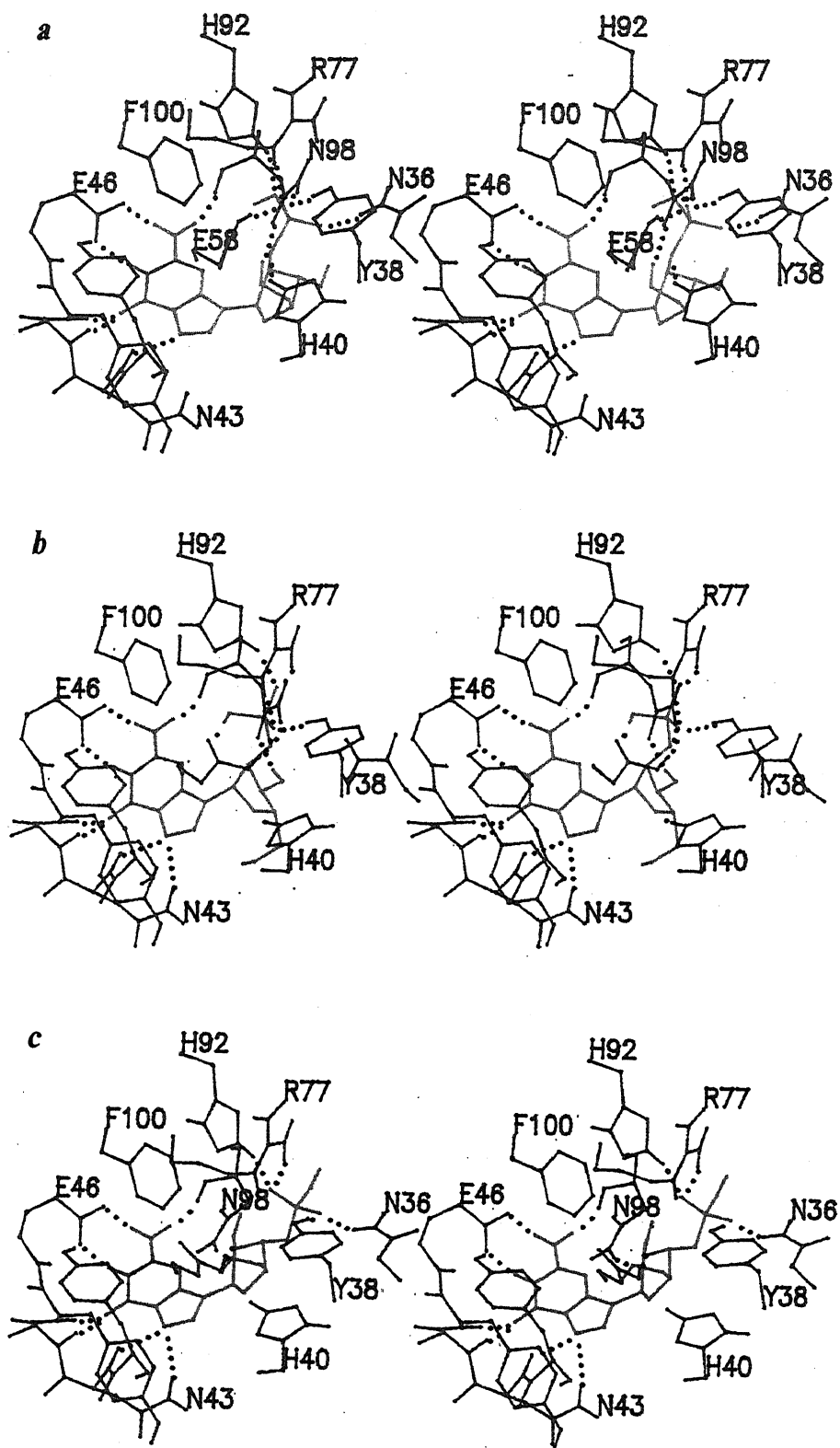
Figure 4. Stereo diagrams of the active-site residues and the inhibitor in the minimum-energy conformations of the complexes of RNase T_1 with the three inhibitors 2'-GMP, 3'-GMP and 5'-GMP. **a,** RNase T_1-2'-GMP (C2'-endo); **b,** RNase T_1-2'-GMP (C3'-endo); **c,** RNase T_1-3'-GMP (C2'-endo); **d,** RNase T_1-3'-GMP (C3'-endo); **e,** RNase T_1-5'-GMP (C2'-endo); **f,** RNase T_1-5'-GMP (C3'-endo). (See next page for figures **d, e, f.**)

endo being more favoured. But the RNase T_1-3'-GMP (C2'-endo) complex has about 8 kcal mol^{-1} higher energy than the RNase T_1-3'-GMP (C3'-endo) complex. Hence 3'-GMP may bind to RNase T_1 predominantly in the C3'-endo form.

The present calculations predict that the glycosyl torsion angle in the RNase T_1-2'-GMP (C2'-endo) complex will be in the +sc (*syn* clinal) range (70°; Table 6), which is in good agreement with the X-ray crystal-structure study[5] of the Lys25-RNase T_1-2'-GMP
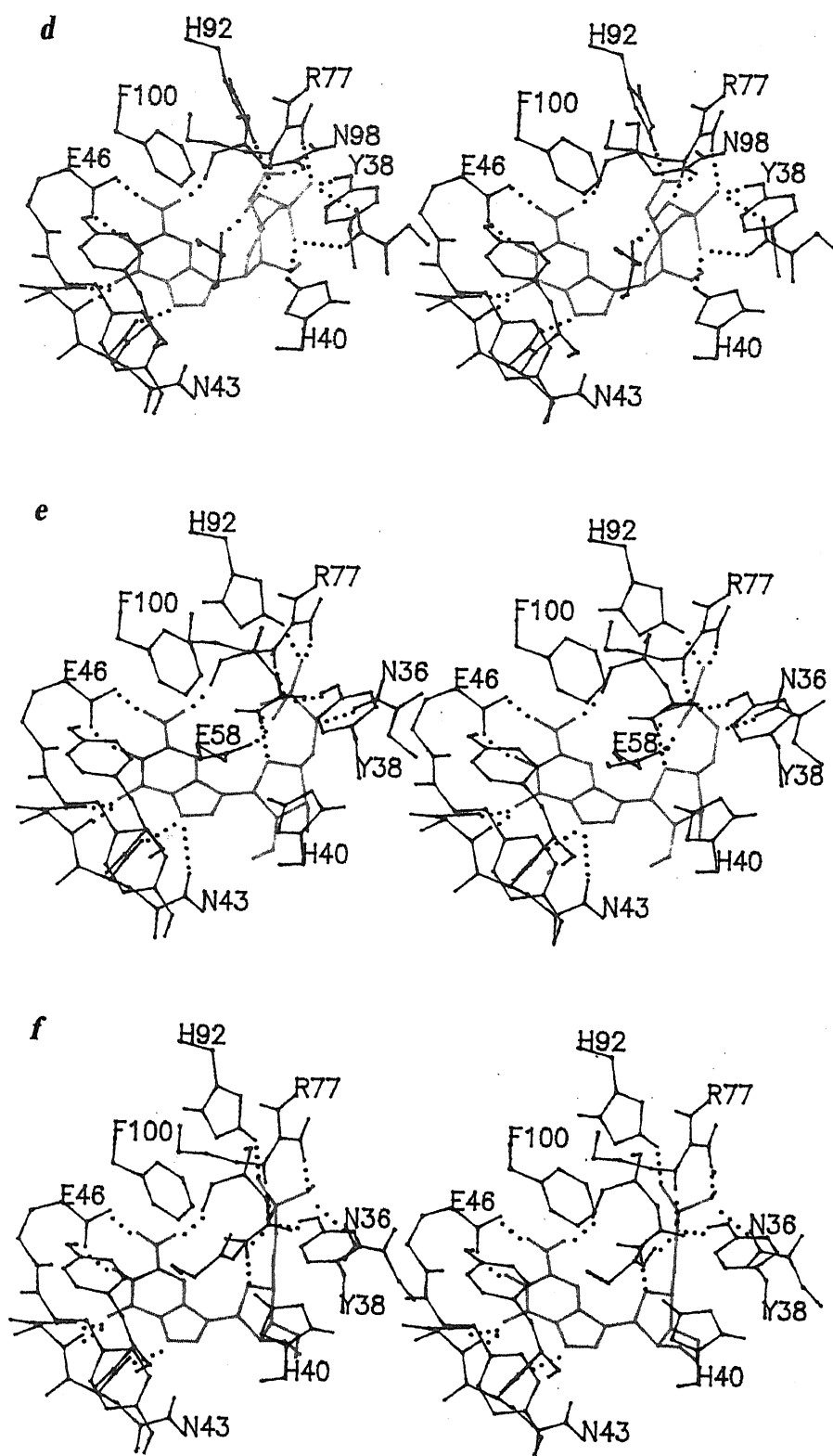
Figure 4. *d–f.*

complex (55°). The same torsion angle in the RNase T_1–2'-GMP (C3'-*endo*) complex falls in the +*ap* (*anti periplanar*) range (157°; Table 6). It is interesting to note that from ^{1}H NMR studies[9], a C3'-*endo syn* conformation was assigned for 2'-GMP in its complex with RNase T_1. The present studies suggest that if the bound 2'-GMP molecule assumes a predominantly C3'-*endo* conformation, the glycosyl torsion angle should be in the +*ap* range and not in the +*syn* range. On the other hand, a +*syn* conformation is possible for the

Table 7. Proposed hydrogen-bonding scheme in the RNase T_1–GMP complexes.

Pucker	C2'-endo			C3'-endo		
Ligand	2'GMP	3'-GMP	5'-GMP	2'-GMP	3'-GMP	5'-GMP
Guanine						
N1H	E46 OE1	E46 OE1	E46 OE1	E46 OE1	E46 OE1	E46 OE1
N2H1	N98 O	N98 O	N98 O	N98 O	N98 O	N98 O
N2H2	E46 OE2	E46 OE2	E46 OE2	E46 OE2	E46 OE2	E46 OE2
O6	N44 N-H	N44 N-H	N44 N-H	N44 N-H	N44 N-H	N44 N-H
	Y45 N-H	Y45 N-H	Y45 N-H	Y45 N-H	Y45 N-H	Y45 N-H
N7	N43 N-H	N43 N-H	N43 N-H	N43 N-H	N43 N-H	N43 N-H
	N43 HD21	N43 HD21	N43 HD21	N43 HD21		
Ribose						
O2'	H40 HE2	E58 HE2		N98 HD22		
O3'H				N98 OD1		
O4'			N98 HD22	H40 HE2		N98 HD22
O5'		N98 HD21	N36 HD21		H92 HE2	
O5'H	N98 OD1				N98 OD1	
Phosphate						
O1	N36 HD21	N36 HD21	N98 HD22	R77 HH21	N36 HD21	Y38 HH
		Y38 HH		H92 HE2	Y38 HH	E58 HE2
					R77 HH21	R77 HE
O2	Y38 HH	R77 HH21	R77 HH21	Y38 HH	N36 HD22	H92 HE2
	E58 HE2	H92 HE2	H92 HE2	E58 HE2	H40 HE2	
	R77 HE			R77 HE		
O3	H92 HE2		Y38 HH		R77 HE	N36 HD22
	N98 HD22		R77 HE			R77 HH21
O3H			E58 OE1	E58 OE1	E58 OE1	

Amino-acid residues of RNase T_1 are indicated by the single-letter code for amino acids and the residue number.

glycosyl torsion angle only when the ribose is in C2'-endo pucker form. Thus the conclusion drawn from ^{1}H NMR studies on the RNase T_1–2'-GMP complex, that the ribose moiety of the bound inhibitor exists entirely in C3'-endo pucker form, may not be correct in view of the results obtained from the present calculations.

The present calculations predict that the inhibitor 3'-GMP preferably adopts a C3'-endo syn conformation when bound to the enzyme (Table 6), in agreement with the conclusions drawn from the ^{1}H NMR studies. On the other hand, in the RNase T_1–5'-GMP complex, the glycosyl torsion angle favours a value in the $-sc$ range ($-76°$ and $-69°$ when the ribose moiety is in C2'-endo and C3'-endo pucker forms respectively). This is in agreement with the conclusions drawn from 2D NMR studies[24], but differs from the earlier ^{1}H NMR study[9], which suggested an anti conformation.

In conclusion, the results obtained from the present calculations are in agreement with experimental studies showing that the inhibitory power decreases in the order 2'-GMP > 3'-GMP > 5'-GMP. They also explain the high pK_a value observed for Glu-58 in the RNase T_1–2'-GMP complex. The apparent discrepancies in the conclusions drawn by different X-ray crystallographic studies and the spectroscopic studies on RNase T_1–2'-GMP complex have been explained by the present calculations. It is shown that 2'-GMP and 5'-GMP can bind to RNase T_1 in either of the ribose puckered conformations whereas 3'-GMP binds to

RNase T_1 predominantly in the C3'-endo puckered conformation.

1. Takahashi, K., J. Biochem., 1985, **98**, 815.
2. Egami, F., Oshima, T. and Uchida, T., Mol. Biol. Biochem. Biophys., 1980, **32**, 250.
3. Takahashi, K. and Moore, S., Enzymes, 1980, **15**, 435.
4. Heinemann, U. and Hahn, U., in Protein–Nucleic Acid Interaction (eds. Saenger, W., and Heinemann, U.), Topics in Molecular and Structural Biology, vol. 10, Macmillan Press Ltd, London, 1989, p. 111.
5. Arni, R., Heinemann, U., Tokuoka, R. and Saenger, W., J. Biol. Chem., 1988, **263**, 15358.
6. Sugio, S., Amisaki, T., Ohishi, H. and Tomita, K., J. Biochem., 1988, **103**, 354.
7. Hoffmann, E., Schmidt, J., Simon, J. and Rueterjans, H., Nucleosides Nucleotides, 1988, **7**, 757.
8. Sugio, S., Oka, K., Ohishi, H., Tomita, K. and Saenger, W., FEBS Lett., 1985, **183**, 115.
9. Inagaki, F., Shimada, I. and Miyazawa, T., Biochemistry, 1985, **24**, 1013.
10. Balaji, P. V., Saenger, W. and Rao, V. S. R., Biopolymers, 1990, **30**, 257.
11. Weinger, S. J., Kollman, P. A., Case, D. A., Singh, U. C., Ghio, C., Alagona, G., Profeta, Jr., S., and Weiner, P., J. Am. Chem. Soc., 1984, **106**, 765.
12. Weiner, S. J., Kollman, P. A., Nguyen, D. T. and Case, D. A., J. Comp. Chem., 1986, **7**, 230.
13. Shanno, D. F., Math. Opr. Res., 1978, **3**, 244.
14. MacKerell, Jr., A. D., Rigler, R., Nilsson, L., Hahn, U. and Saenger, W., Biophys. Chem., 1987, **26**, 247.
15. MacKerell, Jr., A. D., Nilsson, L., Rigler, R. and Saenger, W. Biochemistry, 1988, **27**, 4547.

16. MacKerell, Jr., A. D., Rigler, R., Nilsson, L., Heinemann, U. and Saenger, W., *Eur. Biophys. J.*, 1988, 16, 287.
17. MacKerell, Jr., A. D., Nilsson, L., Rigler, R., Heinemann, U. and Saenger, W., *Proteins: Struct., Funct. Genet.*, 1989, 6, 20.
18. MacKerell, Jr., A. D., Nilsson, L., Rigler, R., Heinemann, U., Hahn, U. and Saenger, W., in *Structure and Chemistry of Ribonucleases*, Proceedings of the first international meeting (eds Pavlovsky, A. and Polyakov, K.), Moscow, 1988, pp. 242.
19. Kostrewa, D., Choe, H.-W., Heinemann, U. and Saenger, W., *Biochemistry*, 1989, 28, 7592.
20. Walz, Jr., F. G. and Hooverman, L. L., *Biochemistry*, 1973, 12, 4846.
21. Campbell, M. K. and Ts'o, P. O. P., *Biochim. Biophys. Acta*, 1971, 232, 427.
22. Takahashi, K., *J. Biochem.*, 1972, 72, 1469.
23. Oshima, T. and Imahori, K., *J. Biochem.*, 1971, 69, 987.
24. Shimada, I. and Inagaki, F., *Biochemistry*, 1990, 29, 757.

RESEARCH COMMUNICATIONS

Dielectric relaxation of non-rigid polar molecules and their mixtures in 1:4 dioxane

Rashmi Arya, Chhavi Aggarwal, J. M. Gandhi and M. L. Sisodia
Department of Physics, Rajasthan University, Jaipur 302 004, India

The dielectric constant and loss factor of the non-rigid polar molecules of o-chloronitrobenzene (I) and 2-chloro-5-aminobenzotrifluoride (II) and their binary mixtures have been measured in dilute solutions of 1:4 dioxane at 9.93 GHz over the temperature range 25–55°C. The dielectric data have been used to determine the relaxation times and thermodynamic parameters for the activated state. The relaxation behaviour of the mixtures is found to be the resultant of the relaxation times of its components, suggesting a simple overlap of the individual dispersion regions. The relaxation times of the mixtures have also been obtained and compared with the values computed using various theoretical formulations. The results indicate that none of the formulae used can predict the experimental results to a satisfactory degree.

THE dielectric relaxation behaviour of binary polar mixtures, as suggested by Schallamach[1], and other workers[2,3], in which both the components are either associated or non-associated, is much different from that of mixtures in which one component is associated and the other non-associated. Besides, dielectric absorption studies have indicated that the relaxation behaviour of polar molecules depends not only on their own interactions but also on their characteristic interaction with the solvent molecules. It therefore seems worthwhile to examine the dielectric relaxation of mixtures of two different polar compounds in a solvent like 1:4 dioxane, which shows hydrogen bonding with various anilines[4,5]. The present study deals with the relaxation behaviour of mixtures of o-chloronitrobenzene (I) and 2-chloro-5-aminobenzotrifluoride (II) with various compositions in 1:4 dioxane at temperatures in the range 25–55°C. Both compounds are non-rigid and polar; I is non-associative and II is weakly associative in

character. There exists a finite possibility of hydrogen bonding between II and 1:4 dioxane.

The relaxation time (τ_0) has been determined following the method of Higasi[6], using the experimental technique of Heston *et al.*[7] The thermodynamic parameters have been calculated using Eyring's[8] theory of rate process. Compounds I and II (Fluka) were used as supplied; 1:4 dioxane (AR grade) was purified by the usual methods.

The values of most probable relaxation time τ_0 listed in Table 1 for three compositions of the mixture and at four temperatures lie between those of the individual components, but vary with the concentration ratio of the components. For resolution of two distinct relaxation processes Davidson[9] suggested that the relaxation time of one component should be 5.8 times that of the other. However, in the present case, the ratio of most probable relaxation times of I and II is much less than 6, thus separate loss maxima are not likely to appear. Thus apparent single relaxation time can be assumed to represent the true behaviour of the mixture systems. The τ_0 value is found to increase with increase in mole fraction of II but the gradient of increase is not linear. As the mole fraction of II increases beyond 0.44 a sharp increase in τ_0 is observed. This increase is evident from the structure of II, where the presence of $-NH_2$ group facilitates hydrogen bonding between hydrogen of $-NH_2$ group and oxygen of 1:4 dioxane, such that, with an increase in the mole fraction of II in the mixture, the association between solute and solvent increases. Studies of microwave absorption by Deogaonkar *et al.*[10,11] indicated formation of complexes through hydrogen bonding in some binary liquid mixtures of chlorophenol with various compounds like toluidine, anilines, etc. They observed a prominent maximum in the tanδ–concentration curve for these compounds and attributed the results to an association between the two types of molecules. However, in the present case, the tanδ–concentration curves are more or less linear at all temperatures. Thus the relaxation behaviour of each mixture studied here is the resultant of the relaxation times of its components, suggesting a